A Novel Two-Dimensional Tactile Slip Display: Design, Kinematics and Perceptual Experiments

ROBERT J. WEBSTER, III, TODD E. MURPHY, LAWTON N. VERNER, and ALLISON M. OKAMURA
Johns Hopkins University

A novel two-degree-of-freedom tactile display reproduces the sensations of sliding contact and incipient slip through the rotation of a ball positioned under the user's fingertip. A pair of motor-driven wheels actuates the ball via contact friction. Mechanical performance requirements are used to define the dimensions and construction method of the device. Kinematic analysis shows that the drive wheel angles and their contact locations with the ball must be carefully selected in order to accurately control the axis of rotation and speed of the ball. However, psychophysical experiments indicate that some kinematic error is tolerable; errors of up to 20° in slip angle and 30% of a nominal velocity may be applied without detection from an average user. The lightweight, modular tactile display was attached to a multi-degree-of-freedom kinesthetic interface and used to display virtual environments with slip. Experimental results demonstrate that users complete a virtual paper manipulation task with lower applied forces using combined slip and force feedback in comparison with conventional force feedback alone.

Categories and Subject Descriptors: H.1.2 [**Models and Principles**]: User/Machine Systems—*Human information processing*; H.5.1 [**Information Interfaces and Presentation**]: Multimedia Information Systems—*Artificial, augmented, and virtual realities*; H.5.2 [**Information Interfaces and Presentation**]: User Interfaces—*Haptic I/O*

General Terms: Design, Experimentation, Human factors, Performance

Additional Key Words and Phrases: Haptic interface, incipient slip, tactile display, psychophysics, virtual reality

1. INTRODUCTION

The sense of touch plays a crucial role in our perception of the world and our performance of identification, manipulation, and grasping tasks. Tactile sensations are felt through a variety of modalities. For example, humans often tap, rub, or envelop objects during exploration. The quality of virtual reality and teleoperated systems relies in part on accurate haptic representations of relevant objects in the environment. While kinesthetic force feedback is widely used in these applications, tactile sensations are often lacking because there exist many challenges in the design and construction of accurate and transparent tactile displays.

One tactile sensation that has proven useful in grasp force modulation is the sensation of objects slipping across the finger, including the initial incipient slip condition. We present the design and evaluation of a novel device for displaying sliding contact at a fingertip in two degrees of freedom (DOF). The device creates tactile slip sensations by means of an actuated ball placed under the fingertip,

Author's address: Department of Mechanical Engineering, The Johns Hopkins University, 223 Latrobe Hall, 3400 North Charles Street, Baltimore, MD. 21218; email: {robert.webster,tmurphy,lverner,aokamura}@jhu.edu.
This work was supported in part by NDSEG Fellowships to Robert J. Webster, III and Lawton N. Verner, and the Johns Hopkins University.

and can be used as a modular attachment to a multi-DOF kinesthetic (force feedback) interface. This combined slip and force feedback display enables a richer set of exploratory procedures [Klatzky and Lederman 1990] to be performed in virtual or teleoperated environments than is possible with a kinesthetic device alone. Psychophysical experiments indicate that the performance of our device is sufficient for realistic haptic display. Experiments using the device in conjunction with a virtual environment have demonstrated improvement in user force modulation in a delicate manipulation task. The feel of the slip sensation under the fingertip has also garnered positive qualitative feedback from users.

We begin in Section 1.1 by outlining relevant results and systems in the literature, and proceed in Section 2 to discuss the design of the slip display. Then, in Section 3, we examine the kinematics of the slip display and discuss drive wheel placement considerations. Section 4 presents the results of psychophysical experiments designed to assess the effects of kinematic considerations and also of using nonidealized physical components on user slip perception. Section 5 examines the results of an experiment demonstrating how the slip display can improve user performance in a delicate manipulation task. Section 6 provides general conclusions and future work.

1.1 Previous Work

Given the importance of human slip sensing for manipulation and exploration, first explored in the physiology literature by Johanson and colleagues [1984] and later by Flanagan and colleagues [1994, 1995, 1997], (an overview of which can be found in Johansson [1998]), it is no surprise that there has been active research in the areas of robotic slip sensing and control. Many different groups, for example, Tada et al. [2001, 2002], Melchiorri [2000], Canepa et al. [1998], Son et al. [2004], and Tremblay and Cutkosky [1993], have developed tactile sensors to detect slip and incipient slip conditions at the surface of robot fingers. (For an overview of early work in this area, see Howe [1994].) Some of these groups have also used slip information collected from tactile sensors, combined with computer control, to modulate the grip force of robotic manipulators. Examples include Tremblay and Cutkosky [1993] and Melchiorri [2000]. This idea was originally proposed in Salisbury [1984], and a discussion of tactile sensing to improve the grasp of robotic fingers can be found in Bicchi et al. [1989]. As these researchers have demonstrated, tactile slip feedback enables a computer-controlled robot to safely handle very delicate objects without either dropping or crushing them. However, a way to display this tactile slip feedback to a human, in order to obtain a corresponding benefit in teleoperation or virtual environments, has not been available. This idea serves as the motivation for our work.

Much of the prior work on displaying tactile information to a human has focused on other sensations such as vibration, temperature, texture, or geometry. Of these, texture and geometry are often displayed using haptic devices employing an array of actuated point contacts. A good overview of this can be found in Wagner et al. [2004]. Pin arrays have been used to present sliding texture to the fingertip [Ikei et al. 1997], and in Ikei and Shiratori [2002] a low-resolution pin array was attached to a kinesthetic haptic display for combined force and tactile feedback. However, this device included only a few pins, with pin spacings too far apart for transparency (greater than specified by the 2-point discrimination test), as noted by the authors. Pin arrays with a larger number of pins are difficult to use in this application due to inherent difficulty constructing drive mechanisms that are small and lightweight. Probably because of this, Kyung et al. [2004] attached their similar 6×1 pin array to a 2-DOF haptic mouse rather than a 3-DOF device like the PHANTOM. The authors are aware of no instances in which such pin-array displays have been used to enhance grip force control. While it may be possible to display slip and incipient slip in this context using such devices, algorithms for doing so have yet to be developed. Any such algorithms will require careful study and validation to determine how successfully pin array devices are able to re-create the natural fingertip sensations associated with slip and incipient slip.

Recent work also provides some other examples of tactile displays attached to larger kinesthetic haptic devices. Feller et al. [2004] attached a pin array a teleoperated robot for palpation experiments. The effect of a rolling ball on the fingertip was studied in Provancher et al. [2003]. In contrast to the system we present, the ball in that system does not slide with respect to the finger, but displays a moving point contact. There is also a link between our work and studies on tactile illusions, for example, Bicchi et al. [2003]. Understanding and exploiting these effects could lead to alternative strategies for controlling our device.

Foundational research on understanding the surface properties and neural codes associated with slip perception at the fingertip can be found in Srinivasan et al. [1990]. In that work, it was found that slip perception is greatly improved when the surface has barely detectable micrometer-sized features, rather than near-perfect smoothness. Birznieks and colleagues [2001] have contributed substantially to understanding the response of fingertip mechanoreceptors, especially with regard to the direction of stimulation. Birznieks has also analyzed the human response to unpredictable frictional changes when performing a two digit manipulation task [Birznieks et al. 1998]. This research provides insight on the processes and control systems within the human, with respect to slip at the fingertip, when manipulating objects. It provides us with intuition about how haptic slip stimulation of these structures in teleoperated or virtual tasks may be perceived and acted upon by users.

There are a few examples of previous work on the development of devices for displaying sliding contact, but all have been 1-DOF devices. Johnson and Phillips [1998] used a 1-DOF system for administering neuroscience experiments. Salada et al. [2002a, 2002b, 2004] developed a 1-DOF bench-top device for slip display and demonstrated that sensations can be displayed on their device with enough fidelity to make it perceptually comparable to sliding one's finger across a real surface. Chen and Marcus [1994] also developed a 1-DOF device for displaying sliding contact to a fingertip.

Psychophysical experiments on slip angle with respect to the fingertip as well as slip velocity have been performed by Salada et al. [2004]. They obtain a just noticeable difference (JND) for slip angle, as well as Weber fractions for several slip velocities at the fingertip. In contrast, our slip angle experiment obtains an absolute threshold for slip angle detection. Rather than investigating JND of constant slip velocity, we examine user perception of time-varying velocities by overlaying sinusoidal variations on a constant velocity signal.

2. SLIP DISPLAY DESIGN

The slip display, shown in Figures 1 and 2, consists of a spherical ball supported under the user's fingertip. The user contacts a portion of the ball through an aperture in the mechanism housing. Two orthogonal wheels actuate the ball and create relative motion between the surface of the ball and the user's fingertip. The device connects to a 3-DOF PHANTOM haptic display (SensAble Technologies, Inc.) through a passive gimbal linkage. The following sections describe mechanical design specifications and considerations.

2.1 Specifications

To smooth integration with a kinesthetic haptic display and maximize transparency, we sought to minimize the size and weight of the device. However, there is a fundamental trade-off between miniaturization and perception of a flat sliding contact surface. As ball diameter is reduced, the contact area with the fingertip becomes smaller and at the limit approaches a point contact. However, a larger ball requires a proportional increase in the size and weight of the device. A 25.4 mm diameter sanded Delrin ball was selected as the object to contact the finger, and the rest of the mechanism was designed around this centerpiece.

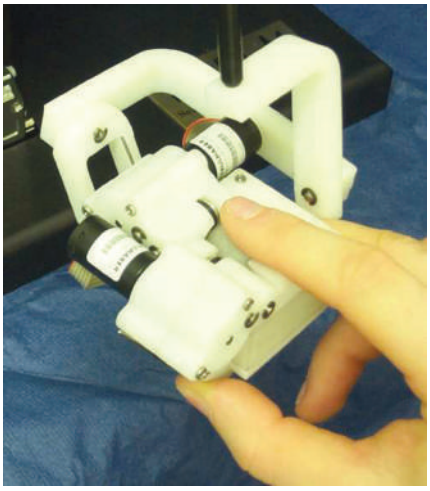

Fig. 1. The two-degree-of-freedom slip display mounted on the output link of a PHANTOM haptic device.

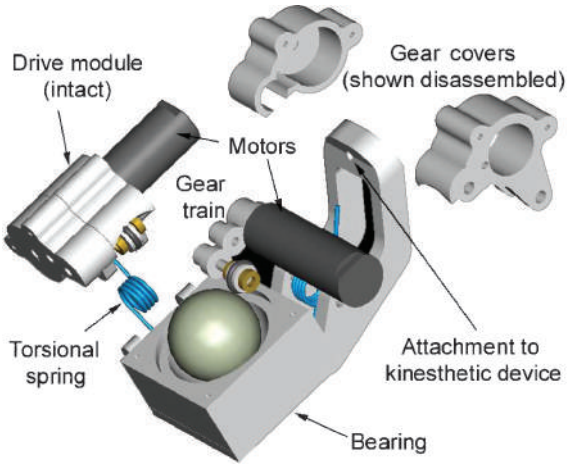

Fig. 2. An exploded view of the device assembly shows the various parts of the tactile slip display.

Determining the necessary driving torque requires an estimate of the normal force applied by a user to the ball. Qualitative experiments were conducted by pushing on a scale with a force comparable to that used when sliding across a surface to assess its texture. These experiments resulted in a maximum normal force estimate of 1.5 N. Another required parameter was the coefficient of friction between the fingertip and the surface of the sanded Delrin ball. Several sources (e.g., Bucholz and Frederick [1988]) suggested a coefficient of $\mu = 0.5$ as a reasonable estimate. Combining these specifications with a drive wheel diameter of 5 mm led to a torque requirement of 3.75 mNm at the drive wheels. An additional important specification for motor selection was the maximum speed across the surface that the a human is likely to use in exploration. It is reasonable to assume that typical hand speeds for users of kinesthetic haptic devices remain well under 30–40 cm/s during normal use. The research of Salada et al. suggests that the size of the aperture where the fingertip contacts the ball will affect user slip perception [Salada et al. 2002a]. Using this reference and qualitative testing, a 15 mm diameter aperture was selected for the fingertip contact interface.

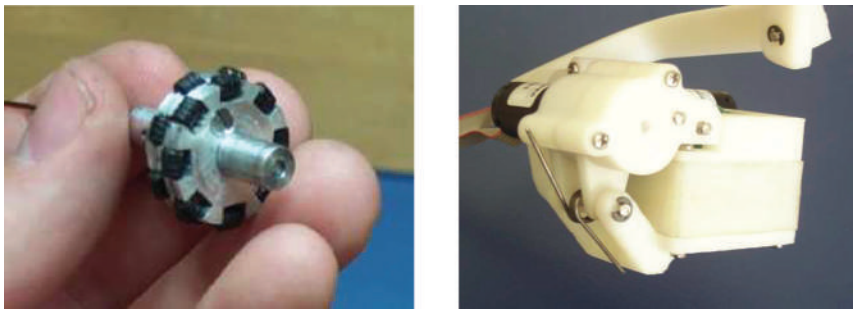

Fig. 3. (Left) The omniwheel from Murphy et al. [2004]. (Right) The drive wheel modules are spring-loaded against the ball.

2.2 Design

Two orthogonal wheels actuate the ball, which in turn imparts the slip sensation to the finger. The ball is supported by low-friction rolling contact in a special bearing developed for the slip display. This bearing consists of a hemispherical pocket lined with ball bearings, around the top edge of which is a bearing race. The bearing is designed to allow the steel ball bearings to roll under the large Delrin ball until they reach the race, where they are pushed around the rim and returned to the area beneath the Delrin ball. As suggested by the design of devices with a similar architecture (see Section 3), one optimal placement choice for each drive wheel is on the axis of rotation created by the other wheel. This arrangement minimizes the friction generated by each wheel during rotation of the other wheel. However, when both wheels turn simultaneously, this arrangement still requires that some slip occur at the wheel–ball interface. This is because these are physical wheels, and the contact with the ball is an area rather than an idealized point contact.

Our bearing design did not permit placement of the drive wheels in this particular optimal configuration, since the bearing supports the entire lower half of the ball. We note that one possible solution to this is "omniwheels" (wheels that impart forces tangential to the wheel's rim, yet present little impedance to motion normal to the disk of the wheel), we found in previous work that it is difficult to manufacture such wheels at this small scale [Murphy et al. 2004]. Consequently, the final design incorporates drive wheels that are solid cylinders with rubber O-rings stretched around the perimeter to produce a high-friction contact with the ball. Section 3 discusses both the desirable and undesirable effects of drive wheel placement and orientation in detail.

Two motors apply torque to the drive wheels through a gear train. The motors selected are capable of 6.75 mNm of torque at the output shaft, and a maximum speed of 9900 rpm. Speed reductions in the gearhead and the gear train mechanism limit the ball speed to 4.88 rev/s, corresponding to a maximum slip speed of about 39 cm/s. To account for tolerances in the assembly and to provide a consistent normal force between the wheels and the ball, each module containing the drive wheel, gear train, and motor is hinged and loaded against the ball with a torsional spring (Figure 3). The fingertip assembly is connected to a kinesthetic haptic device through a passive gimbal linkage that permits rotation around three axes while maintaining the point of finger contact at a fixed location relative to the kinesthetic device output link. The entire assembly weighs 192 g.

While most kinesthetic haptic devices attempt to isolate motors from the user through capstan drives, the slip display does not require this. In rendering haptic slip sensations, we are concerned mainly with velocity rather than force feedback. Any small vibrations from the motors/gearhead transmitted to the ball in the slip display will probably appear as either small high frequency variation in velocity from the desired velocity or perhaps vibration of the housing itself. Neither of these effects is readily

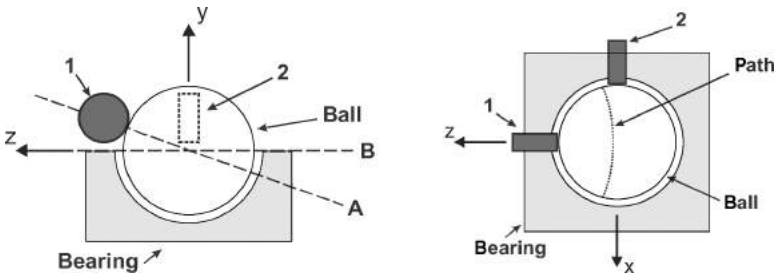

Fig. 4. The positions of the drive wheels (1 and 2) result in additional frictional contact and off-axis ball rotation (axis B is desired and axis A is the result). The path of a point under the user's fingertip is then curved as shown.

apparent to the authors. Further, no adverse effects of using geared motors were reported by device users, who judged the rendered sensations realistic and similar to sliding their finger across a real surface. Our psychophysical experiments, presented in Section 4, examine the absolute threshold of what we believe to be the most important factors to user perception of sliding contact through our slip display. Section 5 also demonstrates that the slip display is capable of improving user performance of a task.

2.3 System Integration

The slip display is integrated with the PHANTOM haptic device and can be used in conjunction with virtual environments created using Microsoft Visual C++ and OpenGL. The PHANTOM and the slip display are controlled using a single computer equipped with a PHANTOM control board and Measurement Computing, Inc. quadrature encoder and D/A boards. The virtual environment graphics are updated at approximately 30 Hz, and the haptic thread runs at 1 kHz.

The position of the end effector (the point where the ball contacts the fingertip) is obtained from the encoders on the PHANTOM, filtered, and differentiated to yield the velocity of the end effector. When the user is moving along a flat surface, the linear velocity of the surface passing under the user's finger (and the corresponding angular velocity of the ball) is proportional to the velocity of the user's fingertip, but in the opposite direction. This is accomplished using a proportional-integral (PI) velocity controller. The integral term includes an antiwindup mechanism that considers the previous 100 samples. The controller was implemented in this way so that the velocity of the ball quickly becomes proportional to the user velocity, while small steady-state position errors are unimportant.

3. ANALYSIS OF DRIVE WHEEL PLACEMENT

Several systems with mechanical topologies similar to our device (a central sphere driven by rolling wheels or disks) have been developed, analyzed, and reported in the literature. A force-feedback trackball was reported in Engel et al. [1994], and a "cobot" has been developed to provide passive kinesthetic feedback [Moore et al. 1999]. The cobot uses a continuously variable transmission that consists of multiple wheels contacting a central ball [Gillespie et al. 2002], as does Kim et al. [2002]. The force-feedback trackball and the cobot were developed for haptics applications. Nakamura et al. [2000] also developed a similar wheel-ball design to serve as a nonholonomic joint for a robotic manipulator.

In our design, the wheels are located orthogonally to each other and their rotational axes are coplanar, but the point of contact between each wheel and the ball lies above the equator (a great circle in the x–z plane, as shown in Figure 4) of the ball. Some effects of this placement are immediately clear. With only one wheel turning, the other wheel creates a constraint that alters the ball's axis of rotation, changing the path a point on the ball would trace under the user's fingertip, as illustrated in Figure 4. In-depth

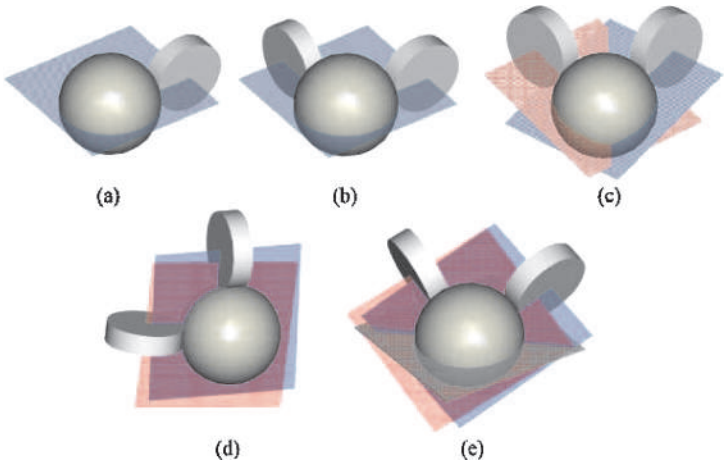

Fig. 5. (a) Considering one wheel only, the axis of rotation of the ball can be anywhere in the plane shown. (b) Wheels on equator share a common plane of permissible axes. (c) Wheels off the equator constrain rotation axis to a line. (d, e) Tilting the drive wheels properly regains 2 DOF motion by realigning constraint planes.

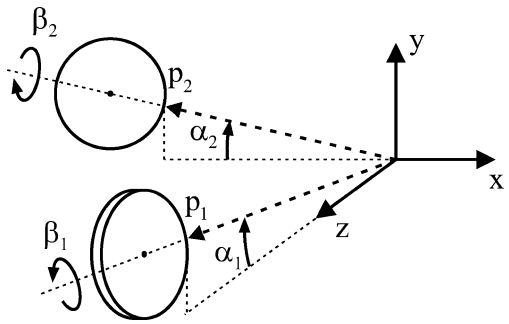

Fig. 6. Angle and vector definitions for the slip display. The two drive wheels are shown, while the ball (omitted from the figure) is centered at the origin.

coverage of constraint types and effects for ball–wheel systems can be found in Nakamura et al. [2001] and Gillespie et al. [2002].

Applying these principles to the slip display, we can consider the constraints on the ball and determine how to command desired contact velocities at the fingertip. In general, a ball has 3 DOF in which it can rotate. A wheel in contact with the ball constrains the ball axis of rotation to 2 DOF. The ball axis of rotation is constrained to lie in the plane defined by the point at the center of the ball and the rotation axis of the wheel. When two wheels contact the ball, the ball axis of rotation depends on the position and orientation of the drive wheels. These constraints are illustrated in Figure 5.

Figure 6 shows the wheel positions. The wheel constraints then lead to the following simple relationship between ball-fingertip contact point velocity and drive wheel input velocity,

$$\begin{bmatrix} v_x \\ v_z \end{bmatrix} = \eta \begin{bmatrix} \sin\alpha \sin\beta & \cos\beta \\ \cos\beta & \sin\alpha \sin\beta \end{bmatrix} \begin{bmatrix} u_1 \\ u_2 \end{bmatrix}, \tag{1}$$

where v_x and v_z are the linear velocities of the ball as it passes under the user's finger, u_1 and u_2 are the drive wheel velocities, and η is the ratio of drive wheel radius to ball radius (a "gear ratio"). The

derivation of this relationship can be found in the Appendix. Taking ω as the ball rotation axis, the derivation also yields the constraint matrix $A(q)$ (where $q = \{\alpha_1, \alpha_2, \beta_1, \beta_2\}$),

$$A(q)\omega = 0, \tag{2}$$

providing a design tool to determine the proper α and β angles. The ideal relationship between α_1, α_2, β_1, and β_2 causes the constraint matrix to become one dimensional (lose rank). This provides a criterion by which the designer can select any two of these angles and solve for the optimal value of the remaining two.

We note that our device does not exactly follow this relationship because of the sub-optimal wheel angles and off-equator placement necessitated by our bearing design. Another source of error is that physical wheels have an area of contact with the ball rather than a point contact. This leads to kinematic creep as described and modeled by Gillespie et al. [2002]. For the slip display as constructed, with $\alpha_1 = \alpha_2 = 15^\circ$ and $\beta_1 = \beta_2 = 0^\circ$, some additional slipping must occur beyond the kinematic creep at each drive wheel for all but one axis of rotation.

While the above sources of wheel slippage error are difficult to model and analyze rigorously, the drive wheels are still able to impart velocities in near-orthogonal directions and the path of the point passing under the user's finger, as shown in Figure 4, is not curved to a large extent.

Users of the device report to us that the perceived feel of the device is similar to that of sliding their finger across a real surface, implying that any kinematic error is below their threshold of detection. To more rigorously demonstrate this, we conducted the following psychophysical experiments.

4. PSYCHOPHYSICAL EXPERIMENTS

Two experiments were performed for the purpose of evaluating the impact of nonideal drive wheel placement and small velocity variation on user perception of the slip display. As illustrated in Figures 4 and 5, drive wheels located off the ball's equator can cause the ball's axis of rotation to exist out of the horizontal plane. Thus, the first experiment evaluates the level at which angular differences in the direction of slip become noticeable to users of the device. Another potential source of non-ideal ball motion is the small variations in velocity introduced by internal mechanism friction or imperfectly round rotating portions of the device. For example, there are finite tolerances for holes drilled in round parts (such as drive wheels and gears). Such manufacturing tolerances could induce periodic variation in the velocity of the ball, even with good control of the motor speed. Thus, the second experiment explores the level at which these types of variations are detectable by the user. Both experiments were conducted using the device shown in Figure 7. This device mimics the tactile interface of the slip display by using a similar lightly sanded Delrin ball and finger aperture. However, this device differs from the 2-DOF slip display in that the ball is directly attached to the shaft of a single encoded motor, ensuring that the ball spins around a known axis at a known angular velocity.

4.1 Angle Discrimination Experiment

We performed an experiment to determine the effect of angular slip direction on perception of sliding contact at the index finger. We placed the test apparatus on a table oriented such that the direction of ball motion simulated the feeling of placing one's finger on a horizontal surface and drawing the finger toward oneself. Twelve subjects (seven male, five female, aged 21–31 years) participated in the experiments. All test participants were familiarized with the device and the intent of the experiment before starting. Each participant was instructed to use the index finger of the right hand to press on the surface of the ball with a light, constant pressure of approximately 0.5 N. Before the start of the experiment, each user was asked to press on a scale until the reading showed 50 g in order to become accustomed to this level of force. The device was aligned so that the axis of rotation was horizontal and perpendicular to the

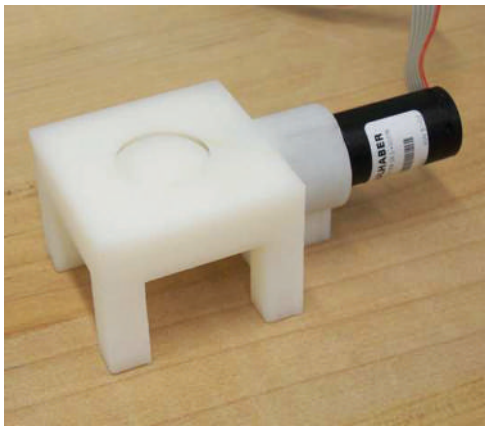

Fig. 7. Single-axis slip device used in psychophysical experiments consisting of a 25.4 mm ball attached to the drive shaft of a motor. The user interacts with the ball in the same manner as in the 2 DOF slip display.

participant's index finger, and the direction of slip was from the finger base to the finger tip. This was identified and presented to the user as the "straight" orientation. The device was then rotated 50° counterclockwise and each user experienced this as an example of an "angled" configuration. Users were then blindfolded and presented with a random sequence of 10 angles ranging from 0–50°, in 5° increments. During the experiment, the ball was spun at approximately 1.25 rev/s, creating a linear slip rate under the fingertip of 10 cm/s. Between presentation of each individual angle, subjects were asked to lift their index finger off the device. Subjects were allowed to feel each angle for as long as they liked, but were instructed not to conduct search activities such as moving their index finger in the horizontal plane or varying contact pressure. For each angle, the subjects verbally selected either "angled" or "straight" as the best description of the sensation they were experiencing. Each angle was presented once to each subject. The order with which the angles were presented was randomized for each subject (using a numerical randomization algorithm) to prevent bias. Subject responses are presented in Figure 8. Note that the bars in this plot roughly follow the classic (s-shaped) psychometric curve. Taking the level where 50% of subjects answered "angled" and 50% answered "straight" yields an absolute threshold of approximately 20°. This indicates that the average user cannot differentiate an angled slip over the fingertip from a straight stimulus up to approximately 20°.

It is very important to note here that this result occurs when the subject's attention is specifically focused on and expecting angled slip. In cases where the subject does not know a priori that the slip direction will be angled, we expect this absolute threshold to be even higher. If graphical visual feedback of a straight slip direction is present, this will probably also contribute to push the threshold still higher. Overall, the results are encouraging for our application, because they suggest that users' perceptual experience is unlikely to be affected by small deviations in slip angle induced by the design considerations and nonidealized physical components that make up the device.

In experiments such as this, factors that may affect the results are the normal force applied (the reason for our training procedure with the scale) and surface texture (as noted in Srinivasan et al. [1990] and Salada et al. [2004]). In contrast to our experiment, which established an absolute threshold for slip angle, the angle experiment in Salada et al. [2004] determined JND of slip angle. There, users were asked to match their perceived angle of slip to a reference angle by actively controlling the angle of slip.

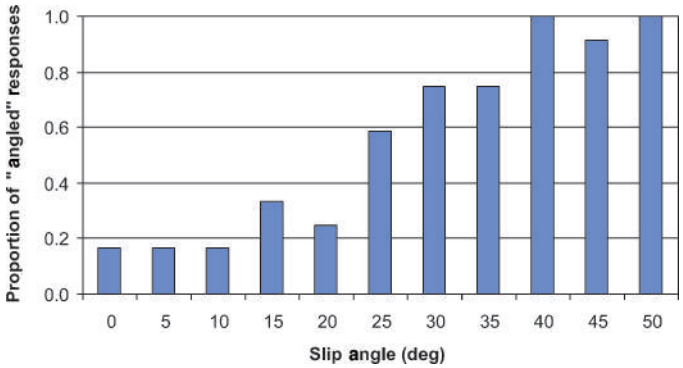

Fig. 8. Subject responses from the angle discrimination experiment show an average angle detection of 20–25°. The proportion of "angled" responses is the number of "angled" responses divided by the total number of responses.

4.2 Velocity Variation Experiment

A second experiment was conducted to determine the level at which humans can perceive sinusoidal variations in the velocity of a sliding contact under their index finger. This experiment was administered with the same device used in the first experiment, and the ball was spun at the same nominal velocity (simulating a 10 cm/s slip speed). Superimposed on this speed was a sine wave with variable amplitude and a constant frequency selected to match the frequency of ball rotation, approximately 1.25 Hz. The amplitude of the sine wave was varied as a ratio of the nominal (mean) speed. When the ratio was zero, the slip speed was a constant 10 cm/s. When the ratio was 1.0, the speed of slip varied sinusoidally between 0 and 20 cm/s. Subjects interacted with the test device in the same way as in the angle experiment, but were not blindfolded because no visual cues were available to them in this experiment. Participants did wear headphones to eliminate auditory cues provided by sounds from the motor and gearhead as the speed varied. Similar to the angle experiment, subjects were allowed to feel both the zero amplitude and maximum amplitude test cases and were told that they would be presented with a randomly ordered sequence of values in between. Subjects were then presented with 11 values of amplitude in increments of 10% of the nominal velocity and asked to classify each as "varying" or "constant." Each amplitude was presented once to each subject. The order with which the amplitudes were presented was randomized in the same manner as in the angle experiment. Subject responses are presented in Figure 9, showing (again by means of a 50% response level) an absolute threshold amplitude ratio of approximately 0.3. This is the level that can generally be displayed without an average user detecting any velocity variation, even when subjects are specifically attempting to discern this velocity variation.

Another study of slip velocity, determining the JND of velocity magnitude around several nominal values, can be found in Salada et al. [2004]. In contrast to that work, our results apply when the velocity change is not constant, but varies as a sinusoidal function of time.

5. FORCE MODULATION FROM SLIP FEEDBACK

A third experiment was performed using the two-dimensional slip display to investigate the significance of slip perception on human force modulation during a delicate manipulation task. A three-dimensional environment was created to simulate a sheet of paper lying on a table (Figure 10). The virtual environment provided vertical kinesthetic force feedback through the PHANTOM when the user pushed down on the table or paper, and tactile slip feedback through the slip display when the user moved across the

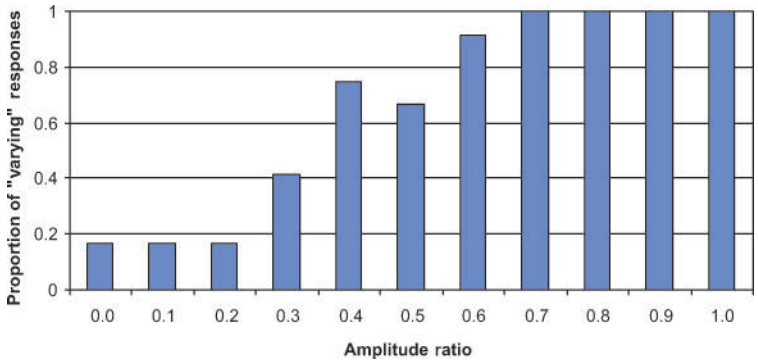

Fig. 9. Subject responses from the slip velocity variation experiment showing average amplitude ratio detection of 30–40% of the nominal velocity. The proportion of "varying" responses is the number of "varying" responses divided by the total number of responses.

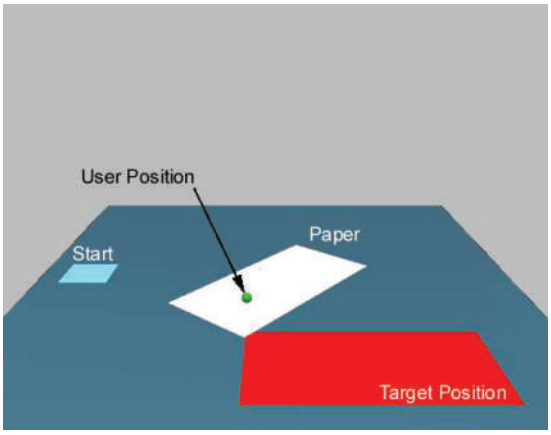

Fig. 10. A screen shot of the virtual environment used in the delicate manipulation task. Users manipulated the paper to the target position with the goal of applying minimum force to the tabletop.

table or paper. When the user contacted the paper with at least 1.5 N of vertical force, the paper would slide and rotate in the plane of the table, following the user's motion.

At the start of an experiment, each element of the virtual environment was described to the user, and the task of translating and rotating the paper from the initial pose to the target pose on the tabletop was explained. Users were instructed to complete the task in a reasonable amount of time, with the primary objective of applying minimum force to the virtual tabletop. The user's finger was then fixed in place via a velcro strap on a small plastic finger rest attached to the front of the slip display. This finger rest maintained the position of the finger over the ball and provided a grip point for the thumb and middle finger. Users were then allowed a brief trial period to become acquainted with the virtual environment and the task. The trial period lasted for approximately 1 minute with slip feedback and 1 minute without slip feedback, and force feedback was provided in both cases.

Users then put on headphones and white noise was played while the task was performed, to ensure that no auditory information could be obtained from device during operation. Each user then

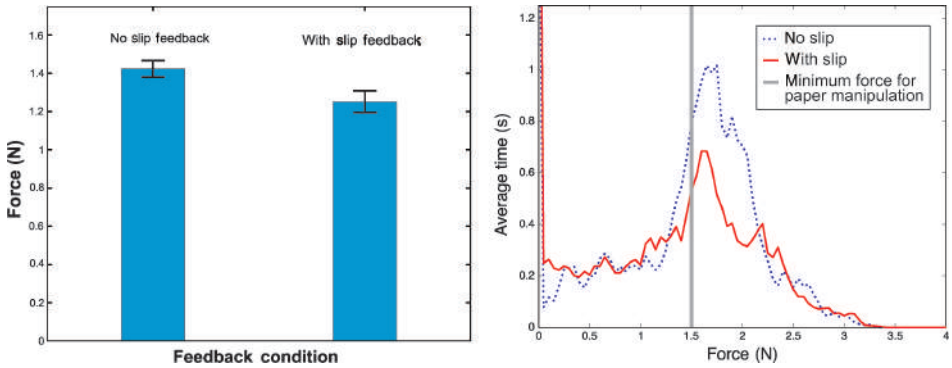

Fig. 11. (Left) Average force used with and without slip feedback with standard error bars. (Right) A force histogram average of all users showing the amount of time spent at discrete force intervals under the slip and no slip conditions. The time spent moving above the table/paper surface is reflected in the large values near 0 N. The vertical line indicates the minimum vertical force at which the finger stops sliding over the surface of the paper and the paper begins to move.

performed the paper manipulation task twice with slip feedback and twice without. The order in which these conditions were presented to each user was randomized, with the constraint that two identical conditions were never presented as the first two conditions to a given user. The results of 10 users are presented here.

Analysis of variance (ANOVA) tests were completed to investigate the effect of slip feedback on operator performance of the paper manipulation task. Two possible criteria quantifying performance improvement are (1) total time to completion and (2) average force applied during the task. Using a significance level of $\alpha = 0.05\%$, we conducted an ANOVA analysis with subject and slip condition (with slip and without slip) included as a factors. Subject was included as a factor because there was significant difference in both time ($p = 0.003$) and average force ($p = 0.004$) between subjects.

Average applied force was reduced significantly with slip feedback ($p = 0.004$), demonstrating that the slip sensation improved subjects' ability to modulate their force accurately, the stated primary objective of the experiment. Figure 11 illustrates the average force and standard error for the two feedback conditions. Although mean completion time was lowered via slip feedback (11.22 s without slip and 10.42 s with slip feedback), the difference was not statistically significant ($p > 0.05$). We expect that, with a more complex and longer-duration task, time to completion could become significant. Another interesting way to look at the data is as a force histogram (Figure 11), showing an apparent difference in the forces users apply near the threshold for moving the paper.

These results, particularly the improved average applied force, demonstrate that the addition of our slip display to a kinesthetic force feedback device can improve user performance in delicate manipulation tasks.

6. CONCLUSIONS AND FUTURE WORK

We have presented a two-dimensional tactile device that displays sliding contact to the user. The slip display, used in conjunction with a force feedback haptic interface (such as the PHANTOM), provides a system capable of accurately rendering both tactile slip and kinesthetic haptic sensations. Anecdotally, users report that the tactile sensations they feel are effective in simulating slip. More rigorous experiments demonstrate that the slip display is able to improve user performance in modulating applied force in virtual environments. This shows that the slip display has the potential to improve performance in virtual and teleoperated manipulation of delicate objects, perhaps eventually obtaining performance

enhancements similar to those demonstrated in the literature on computer-controlled systems that make use of incipient slip feedback for force modulation. We also discussed in detail the design trade-offs and kinematic effects associated with wheel placement and real-world manufacturing tolerances. Psychophysical experiments assessed the effect of these factors on user perception of slip by examining angle and velocity variation detection thresholds.

Future work on device design includes alternate placement of drive wheels as well as investigation of methods for encoding the motion of the ball itself, since motor encoders alone do not account for slippage of the ball relative to the wheels. The slip display also enables investigation of important questions involving the nature and limits of human slip perception. In particular, the ability to decouple slip from proprioception may allow us to explore the contribution each of these sensations to human perception of surface properties.

Appendix: Derivation of Wheel-Ball Velocity Relationship

To derive Eq. (1), we investigate the effect of wheel constraints (as shown in Figures 5 and 6). Let the rotation axis of the ball be denoted ω. As shown in Figure 6, the drive wheels are located at angles α_1 and α_2 above the x–z plane. We define two points p_1 and p_2 located at the points of contact between the ball and the drive wheels as

$$p_1 = r_b \begin{bmatrix} 0 \\ \sin\alpha_1 \\ \cos\alpha_1 \end{bmatrix}, \quad p_2 = r_b \begin{bmatrix} -\cos\alpha_2 \\ \sin\alpha_2 \\ 0 \end{bmatrix}, \tag{3}$$

where r_b is the radius of the ball. Additionally, we define β as the drive wheel orientation angle such that β_1 corresponds to a rotation around the p_1 axis, and β_2 corresponds to a rotation around the p_2 axis.

The wheel constraints prevent the instantaneous velocity of the points p_1 and p_2 from moving in a direction perpendicular to the disk of the corresponding drive wheel. The velocities of each point in the world frame are given by

$$v_{p_1} = \omega \times p_1, \quad v_{p_2} = \omega \times p_2, \tag{4}$$

and the constraints are written as

$$v_{p_1}^T R_x(-\alpha_1) \begin{bmatrix} \cos\beta_1 \\ \sin\beta_1 \\ 0 \end{bmatrix} = 0, \quad v_{p_2}^T R_z(-\alpha_2) \begin{bmatrix} 0 \\ -\sin\beta_2 \\ \cos\beta_2 \end{bmatrix} = 0, \tag{5}$$

where $R_x(-\alpha_1)$ denotes a rotation of $-\alpha_1$ around the x axis and $R_z(-\alpha_2)$ denotes a rotation of $-\alpha_2$ around the z axis. These constraints can be expressed concisely as,

$$\overbrace{\begin{bmatrix} -\sin\beta_1 & \cos\alpha_1\cos\beta_1 & -\cos\beta_1\sin\alpha_1 \\ \cos\beta_2\sin\alpha_2 & \cos\alpha_2\cos\beta_2 & \sin\beta_2 \end{bmatrix}}^{A(q)} \omega = 0. \tag{6}$$

This $A(q)$ is the constraint matrix of the form presented in Murray et al. [1994]. If the matrix A is full row-rank, the system has only one DOF. However, for the right combinations of α_1, α_2, β_1, and β_2, the matrix loses full rank, yielding an additional degree of freedom. In general, if $\text{rank}(A) = 1$, the axis of rotation may be controlled in 2 DOF by appropriate ratios of input wheel velocities. It should be noted that selecting any two of these four angles allows us to solve for the other two.

Deriving the velocity of a point on the ball passing underneath the user's fingertip requires a relationship that maps the drive wheel input velocities to the resulting axis of rotation of the form

$$\omega = u_1 g_1 + u_2 g_2, \tag{7}$$

where u_1 and u_2 are the magnitudes of the input velocities and g_1 and g_2 are the control vector fields. The vectors g_1 and g_2 must lie in the null space of A and should be selected such that they represent the velocity inputs of the two drive wheels. We define vectors d_1 and d_2 as the vectors passing through points p_1 and p_2 tangent to the surface of the ball and in the direction of wheel velocity. The general form of these vectors is

$$d_1 = \begin{bmatrix} -\sin\beta \\ \cos\alpha\cos\beta \\ -\sin\alpha\cos\beta \end{bmatrix}, \quad d_2 = \begin{bmatrix} \sin\alpha\cos\beta \\ \cos\alpha\cos\beta \\ \sin\beta \end{bmatrix}. \tag{8}$$

A natural choice in our system is for g_1 and g_2 to point along the axis of rotation of the drive wheels, defined by

$$g_1 = \frac{r_w}{{r_b}^2}[p_1 \times d_1] = \eta \begin{bmatrix} -\cos\beta \\ -\cos\alpha\sin\beta \\ \sin\alpha\sin\beta \end{bmatrix} \tag{9}$$

$$g_2 = \frac{r_w}{{r_b}^2}[p_2 \times d_2] = \eta \begin{bmatrix} \sin\alpha\sin\beta \\ \cos\alpha\sin\beta \\ -\cos\beta \end{bmatrix} \tag{10}$$

where $\eta = r_w/r_b$. We wish to determine the linear velocity of the point p_3 on the surface of the ball and in contact with the user's fingertip. This point lies at $p_3 = [0\ r_b\ 0]^T$, and its velocity expressed in the world coordinate frame is

$$v_f = (u_1 g_1 + u_2 g_2) \times p_3. \tag{11}$$

Note that the y component of v_f is always zero because of the p_3 contact location. Simplifying Eq. (11) yields the relationship between drive wheel input and the velocity of the point passing under the user's finger found in Eq. (1).

ACKNOWLEDGMENTS

The authors wish to thank Prof. Noah Cowan for judicious and mathematical review and Jake Abbott for conceptual conversations on kinematics and control issues.

REFERENCES

Bicchi, A., Salisbury, J. K., and Dario, P. 1989. Augmentation of grasp robustness using intrinsic tactile sensing. In *IEEE International Conference on Robotics and Automation*, vol. 1, 302–307.

Bicchi, A., Sciling, E. P., and Dente, D. 2003. Tactile flow induced haptic illusions. In *Eurohaptics*, Dublin, Ireland. 314–329.

Birznieks, I., Burstedt, M. K. O., Edin, B. B., and Johansson, R. S. 1998. Mechanisms for force adjustments to unpredictable frictional changes at individual digits during two-fingered manipulation. *Journal of Neurophysiology 80*, 1989–2002.

Birznieks, I., Jenmalm, P., Goodwin, A. W., and Johansson, R. S. 2001. Encoding of direction of fingertip forces by human tactile afferents. *Journal of Neuroscience 21*, 20, 8222–8237.

Bucholz, B. and Frederick, L. J. 1988. An investigation of human palmar skin friction and the effects of materials, pinch force and moisture. *Ergonomics 31*, 3, 317–325.

Canepa, G., Petrigliano, R., and M. Campanella, D. D. R. 1998. Detection of incipient object slippage by skin-like sensing and neural network processing. *IEEE Transactions on Systems, Man, and Cybernetics 28*, 3, 348–356.

CHEN, E. AND MARCUS, B. 1994. Exos slip display research and development. In *Proceedings of the International Mechanical Engineering Congress and Exposition*. ASME DSC, vol. 55–1. 265–270.

ENGEL, F. L., GOOSSENS, P., AND HAAKMA, R. 1994. Improved efficiency through i- and e-feedback: A trackball with contextual force feedback. *International Journal of Human–Computer Studies 41*, 6, 949–974.

FELLER, R. L., LAU, C. K. L., WAGNER, C. R., PERRIN, D. P., AND HOWE, R. D. 2004. The Effect of Force Feedback on Remote Palpation. In *Proceedings of IEEE International Conference on Robotics and Automation*. 782–788.

FLANAGAN, J. R. AND TRESILIAN, J. R. 1994. Grip load force coupling: A general control strategy for transporting objects. *Journal of Experimental Psychology: Human Perception and Performance 20*, 944–957.

FLANAGAN, J. R. AND WING, A. M. 1995. The stability of precision grip forces during cyclic arm movements with a hand-held load. *Experimental Brain Research 105*, 455–464.

FLANAGAN, J. R. AND WING, A. M. 1997. The role of internal models in motion planning and control: Evidence from grip force adjustments during movements of hand-held loads. *Journol of Neuroscience 17*, 1519–1528.

GILLESPIE, R. B., MOORE, C. A., PESHKIN, M., AND COLGATE, J. E. 2002. Kinematic creep in continuously variable transmissions: Traction drive mechanics for cobots. *Journal Mechanical Design 124*, 4 (Dec.), 713–722.

HOWE, R. D. 1994. Tactile sensing and control of robotic manipulation. *Journal of Advanced Robotics 8*, 3, 245–261.

IKEI, Y. AND SHIRATORI, M. 2002. TextureExplorer: A tactile and force display for virtual textures. *Haptic Interfaces for Virtual Environment and Teleoperator Systems*, 327–334.

IKEI, Y., WAKAMATSU, K., AND FUKUDA, S. 1997. Texture presentation by vibratory tactile display-image based presentation of a tactile texture. In *Virtual Reality Annual International Symposium*, 199–205.

JOHANSSON, R. S. 1998. Sensory input and control of grip. *Novartis Foundation Symposium 218*, 45–59.

JOHANSON, R. S. AND WESTLING, G. 1984. Roles of glabrous skin receptors and sensorimotor memory in automatic control of precision grip when lifting rougher or more slippery objects. *Experimental Brain Research 56*, 550–564.

JOHNSON, K. O. AND PHILLIPS, J. R. 1988. A rotating drum stimulator for scanned embossed patterns and textures across the skin. *Journal of Neuroscience Methods 22*, 221–231.

KIM, J., PARK, F. C., PARK, Y., AND SHIZUO, M. 2002. Design and analysis of a spherical continuously variable transmission. *ASME Journal of Mechanical Design 124*.

KLATZKY, R. L. AND LEDERMAN, S. J. 1990. Intelligent exploration by the human hand. In *Dextrous Robot Hands*, S. T. Venkataraman and T. Iberall, Eds. Springer-Verlag, Berlin, 66–81.

KYUNG , K.-U., SON, S.-W., KWON, D.-S., AND KIM, M.-S. 2004. Design of an Integrated Tactile Display. In *Proceedings of IEEE International Conference on Robotics and Automation*. 776–781.

MELCHIORRI, C. 2000. Slip detection and control using tactile and force sensors. *IEEE/ASME Transactions on Mechatronics 5*, 3, 235–242.

MOORE, C. A., PESHKIN, M. A., AND COLGATE, J. E. 1999. Design of a 3R cobot using continuously variable transmissions. In *Proceedings of IEEE International Conference on Robotics and Automation*.

MURPHY, T. E., WEBSTER, R. J., AND OKAMURA, A. M. 2004. Design and performance of a two-dimensional tactile slip display. In *Eurohaptics*. 130–137.

MURRAY, R. M., LI, Z., AND SASTRY, S. S. 1994. A mathematical introduction to robotic manipulation. In *Dextrous Robot Hands*, S. T. Venkataraman and T. Iberall, Eds. CRC Press.

NAKAMURA, Y., CHUNG, W., AND SRDALEN, O. 2001. Design and control of the nonholonomic manipulator. *IEEE Transactions on Robotics and Automation 17*, 1.

PROVANCHER, W. R., KUCHENBECKER, K. J., NIEMEYER, G., AND CUTKOSKY, M. R. 2003. Perception of curvature and object motion via contact location feedback. In *11th International Symposium on Robotics Research*, Siena, Italy.

SALADA, M. A., COLGATE, J. E., LEE, M. V., AND VISHTON, P. M. 2002a. Fingertip haptics: A novel direction in haptic display. In *Proceedings of the 8th Mechatronics Forum International Conference*. University of Twente, Enschede, Netherlands. 1211–1220.

SALADA, M. A., COLGATE, J. E., LEE, M. V., AND VISHTON, P. M. 2002b. Validating a novel approach to rendering fingertip contact sensations. In *Proceedings of the 10th IEEE Virtual Reality Haptics Symposium*. 217–224.

SALADA, M. A., COLGATE, J. E., VISHTON, P. M., AND FRANKEL, E. 2004. Two experiments on the perception of slip at the fingertip. In *12th Symposium on Haptic Interfaces for Virtual Environments and Teleoperator Systems*. 146–153.

SALISBURY, J. K. 1984. Interpretation of contact geometries from force measurements. In *Robotics Research*, M. Brady and R. Paul, Eds. MIT Press, Cambridge, MA. 565–577.

SON, J. S., MONTEVERDE, E. A., AND HOWE, R. D. 2004. A tactile sensor for localizing transient events in manipulation. In *Proceedings of IEEE International Conference on Robotics and Automation*. 471–476.

Srinivasan, M. A., Whitehouse, J. M., and LaMotte, R. H. 1990. Tactile detection of slip: surface microgeometry and peripheral neural codes. *Journal of Neurophysiology 63*, 6, 1323–1332.

Tada, M., Shibata, T., and Ogasawara, T. 2001. Artificial finger skin having ridges and distributed tactile sensors. *Proceedings of IEEE International Conference on Intellegent Robots and Systems*, 686–691.

Tada, M., Shibata, T., and Ogasawara, T. 2002. Investigation of the touch processing model in human grasping based on the stick ratio within a fingertip contact interface. *Proceedings of IEEE International Conference on Systems, Man and Cybernetics*, vol. 5.

Tremblay, M. R. and Cutkosky, M. R. 1993. Estimating friction using incipient slip sensing during a manipulation task. *Proceedings of IEEE International Conference on Robotics and Automation*, 429–434.

Wagner, C., Lederman, S., and Howe, R. 2004. Design and performance of a tactile shape display using rc servomotors. *Journal of Haptics Research 3*, 4 (Aug.) (www.haptics-e.org).

Received August 2004; revised October 2004; accepted January 2005